

Identification of absorbing galaxies towards the QSO J2233–606 in the Hubble Deep Field South *

Laurence Tresse^{1,2,8}, Michel Dennefeld^{1,3}, Patrick Petitjean^{1,4}, Stefano Cristiani^{5,6}, and Simon White⁷

¹ Institut d’Astrophysique de Paris - CNRS, 98bis Boulevard Arago, F-75014 Paris

² Istituto di Radioastronomia del CNR, Via Gobetti, 101, I-40129 Bologna, Italy

³ Université Pierre et Marie Curie, Paris, France

⁴ DAEC - Observatoire de Paris, 5 Place Jules Janssen, 92295 Meudon

⁵ European Southern Observatory, Karl–Schwarzschild–Str. 2, D-85748 Garching bei München, Germany

⁶ Dipartimento di Astronomia, Università di Padova, Vicolo dell’Osservatorio 5, I-35122 Padova, Italy

⁷ Max Planck Institut für Astrophysik, D-85740 Garching, Germany

⁸ Laboratoire d’Astronomie Spatiale, BP8, F-13376, Marseille Cedex 12

Abstract. We present spectroscopic observations of galaxies lying within 1' from the quasar J2233–606 in the Hubble Deep Field South (HDF-S). Several are found to be coincident in redshift with absorption-line systems seen in the HST QSO J2233–606 spectrum. We detect a new $z_{\text{em}} = 1.335$ quasar with $I = 20.8$ at a projected angular separation of 44.5" (or $200h^{-1}$ kpc) from J2233–606. This makes the QSO pair an ideal target for QSO environment studies. Indeed, strong H I Ly α and Ly β absorptions are seen at $z_{\text{abs}} = 1.3367$ in the spectrum of QSO J2233–606, consistent with a neutral hydrogen column density of $N(\text{H I}) > 10^{16} \text{ cm}^{-2}$. The bright spiral galaxy (J2233378–603324), projected at 4.7" from QSO J2233–606, is at $z = 0.5704$. Strong H I absorption is seen in the QSO spectrum. The paucity of metal absorptions suggests that the disk of this galaxy is metal-poor.

Key words: quasars:individual: J2233–606, Galaxies: ISM, quasars:absorption lines, Galaxies: halo

1. Introduction

The last two years have seen substantial progress in understanding galaxy formation and evolution thanks, in particular, to the data provided by the Hubble Deep Field-North (HDF-N; Williams et al. 1996), which complement, at high-redshift, the data from well-defined ground-based surveys (Gallego et al. 1995 and the CFRS: Lilly et al. 1995). Very recently, a second HST deep field has been observed in the southern hemisphere (HDF-S; Williams et al. 1998). The STIS field was chosen to contain a

Send offprint requests to:

* Based on observations obtained with the NTT at the European Southern Observatory, La Silla, Chile under programs 61.A-0631 and 62.O-0363; and with the NASA/ESA *Hubble Space Telescope* by the Space Telescope Science Institute, which is operated by AURA, Inc., under NASA contract NAS 5-26555.

bright quasar ($V \sim 17.5$, $z_{\text{em}} = 2.24$), J2233–606, selected by Hewett & Boyle (Boyle 1997). Both deep imaging of the QSO field and spectroscopy of the quasar itself have been obtained (Gardner et al. 1999). Low- and high-dispersion spectra have also been obtained already with ground-based telescopes (Outram et al. 1998; Savaglio 1998; Sealey et al. 1998). This set of data offers the unique opportunity to address important questions related to the connection between galaxies and QSO absorption lines including the absorption cross-section of faint galaxies and the structure of the inter-galactic medium over the redshift range 1.2–2.2.

Spectroscopy of the brightest galaxies in the full HDF-S, selected purely according to I-magnitude, has been performed on the ESO-NTT by a collaboration assembled under the auspices of the European Training and Mobility of Researchers (TMR) program. Here we comment on the galaxies closest to QSO J2233–606 and discuss their possible relation with absorption lines identified in the QSO spectrum. The full sample of observed galaxies will be discussed elsewhere (Dennefeld et al. 1999).

Section 2 presents briefly the selection of targets and observations. In Section 3, we describe individual galaxies, and their relevance to features in the QSO spectrum. In Section 4 we draw our conclusions.

2. Selection of targets, observations and data reduction

A 30mn equivalent I-band image centered on the QSO J2233–606 was obtained under ESO Director’s discretionary time with the EMMI-NTT red-imaging channel and made available to us for target selection. Photometric calibration has been done with standard stars from Landolt (1992) and the accuracy of the zero point is better than 0.1 magnitude. Source extraction and star-galaxy separation were performed with Sextractor (Bertin and Arnouts, 1996) resulting in a catalogue of 1159 objects

with $I < 22.2$, complete at the 90% level. The US Naval Observatory catalogue was used as reference for the astrometry resulting in an accuracy close to $1''$ for absolute positions and about three times better for relative positions within the field.

Multi-slit spectroscopy at a spectral resolution of 2.8 \AA per pixel has been performed with EMMI at the ESO-NTT, where about thirty objects can be observed simultaneously. The width of the slitlets was either $1.04''$ or $1.34''$, depending on the seeing conditions, corresponding to about 4 and 5 pixels respectively. The spectral range covers $3900\text{--}10000 \text{ \AA}$ but its actual length depends on the location of the object within the mask. Reduction was done with standard techniques using an updated version of Multired under the IRAF reduction package. Spectra were flux calibrated using standard stars from Stone and Baldwin (1984) with no attempt to correct here for aperture losses.

The spectroscopic survey is nearly complete down to $I = 21.0$ in the full EMMI field ($5.1 \times 8.2 \text{ sq.arcmin}$). Due to MOS punching constraints, and to limited observing time, the sample is not always complete in sub-areas where several galaxies of similar magnitude are lying close to each other. Fainter ones were also sometimes included to fill in the masks. Full details about observations and reductions can be found in Dennefeld et al. (1999).

3. Galaxies around the QSO J2233–606

We discuss here only the objects lying within $1'$ from QSO J2233–606. Identification of galaxies in the field can be found on Figure 1 (extracted from our I-band image). Table 1 gives the running number of our photometric catalogue, the J2000 coordinates (α, δ), the I magnitude, the redshift (z), the projected angular distance (d) in arcsec to QSO J2233–606, and the impact parameter (q) in kpc. Throughout the paper, we adopt $H_0 = 100h \text{ km s}^{-1} \text{ Mpc}^{-1}$ and $q_0 = 0.5$. All redshifts are accurate to ~ 0.001 (except for G1143 where the redshift is still uncertain). We discuss below in more detail objects G486 and Q433.

3.1. Quasar 433 = J2233415–603255

This object is an active galaxy, as shown by its spectrum (see Fig. 2). Its redshift is determined from the broad emission lines $\text{Mg II} \lambda 2799$ and $\text{C III}] \lambda 1909$, giving $z = 1.3352$ and 1.3350 ± 0.001 respectively. Thus $[\text{O II}] \lambda 3727$ falls just outside the red-end of our spectrum. We see also the broad $\text{Fe II } \lambda \lambda 2400, 2600$ complex, and the unidentified broad feature around 2100 \AA usually seen in quasar spectra (see the composite QSO spectrum in Francis et al. 1991). The distance modulus is 43.6, thus the absolute magnitude $M(I) = -22.8$. For a typical $B - I$ colour of 1 magnitude for quasars, we derive $M(B) = -21.8$. This is more characteristic of a Seyfert-1 galaxy as the arbitrary separation between Seyferts and QSO's is at $B = -23$. Since the object appears unresolved on the HST flanking-field image, we call it a quasar.

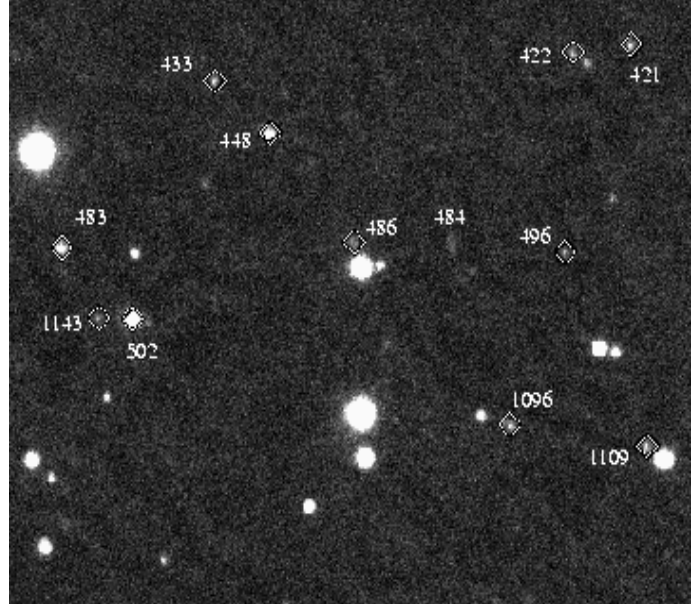


Fig. 1. Galaxies observed around J2233–606 (North is at top, and East to the left). Diamonds indicate objects where spectra are available, with running number as in Table 1.

Galaxy	α	δ	I	z	d	q
G422	338.38343	-60.5473	20.64	0.6465	56"8	220
Q433	338.42273	-60.5487	20.78	1.3351	44"5	190
G448	338.41668	-60.5513	19.55	0.5800	29"8	112
G483	338.43954	-60.5569	19.91	0.3302	58"4	170
G486	338.40752	-60.5567	20.32	0.5704	4"7	18
G496	338.38436	-60.5572	21.48	0.4148	39"9	130
G502	338.43177	-60.5604	18.57	0.2268	45"0	103
G1096	338.39056	-60.5657	20.79	0.4147	40"1	130
G1143	338.43553	-60.5604	21.29	0.066?	51"5	45

3.2. Galaxy 486 = J2233378–603324

This galaxy is particularly interesting since it is projected at only $4.7''$ from the QSO J2233–606. Its spectrum is displayed in Figure 3. The redshift, $z = 0.5704 \pm 0.001$ is determined from $[\text{O II}] \lambda 3727$, $[\text{O III}] \lambda 5007$ and CaK lines. The Balmer break is not conspicuous. The spectrum is consistent with the spiral morphology and the presence of numerous H II regions apparent in the HST image.

4. Absorption lines in the QSO J2233–606

4.1. System at $z_{\text{em}} = 1.3351$ (Quasar Q433)

We searched in the HST spectrum for absorptions around $z_{\text{em}} = 1.3351$. The wavelength ranges of $\text{H I} \text{ Ly}\alpha$ together with $\text{C IV} \lambda \lambda 1548, 1550$ and $\text{N V} \lambda \lambda 1238, 1242$ at $z_{\text{abs}} \sim z_{\text{em}}$, are shown in Figure 4 on a velocity scale. Strong $\text{H I} \text{ Ly}\alpha$ and $\text{Ly}\beta$ absorptions are seen at $z_{\text{abs}} = 1.3367$. The equivalent width of the $\text{Ly}\alpha$ line, $W_{\text{obs}} = 2.31 \text{ \AA}$, is consistent with a neutral hydrogen column density of $N(\text{H I}) > 10^{16} \text{ cm}^{-2}$. The profiles of the $\text{Ly}\alpha$ and $\text{Ly}\beta$ lines are indicative

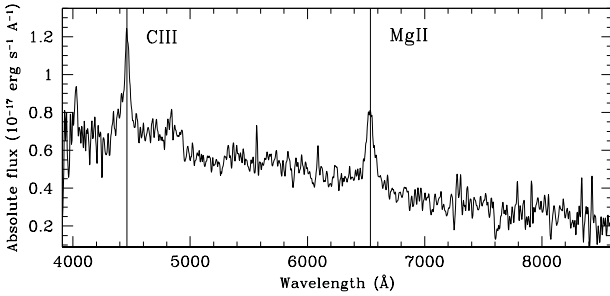


Fig. 2. Spectrum of object 433 = J2233415–603255.

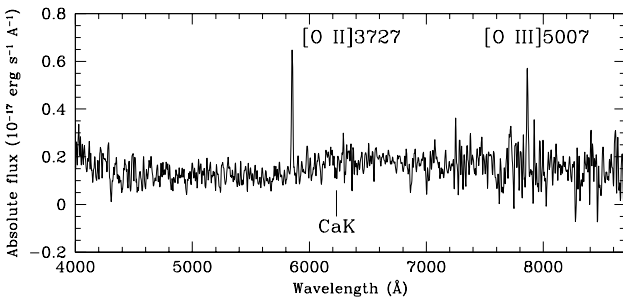


Fig. 3. Spectrum of object 486 = J2233378–603324.

of the presence of two subcomponents at $z_{\text{abs}} = 1.3363$ and 1.3368 ($\Delta v \sim 60 \text{ km s}^{-1}$). The S/N ratio in the Ly β region is not high enough however to be sure of this conclusion. The presence of metals in the cloud is questionable but, if real, supports the presence of several components with different ionization levels. Indeed there is a C IV $\lambda 1548$ component at $\Delta v \sim -60 \text{ km s}^{-1}$ with no obvious C IV $\lambda 1550$ counterpart; the latter could be under the detection limit. Better data in the optical range will help to decide if the C IV doublet is real. There is a N V $\lambda 1242$ component at $\Delta v \sim +55 \text{ km s}^{-1}$ with no associated C IV absorption but, if real, the N V $\lambda 1238$ is blended with a strong Ly α line. An absorption line is seen at the expected position of O VI $\lambda 1031$ but with no obvious O VI $\lambda 1037$ counterpart; the corresponding part of the spectrum has a poor S/N ratio however.

The good coincidence between the QSO redshift and the absorption redshift ($\Delta v \sim 200 \text{ km s}^{-1}$) suggests a physical link between the quasar and the absorber. Indeed, the number density of Ly α lines with $N(\text{H I}) > 10^{16} \text{ cm}^{-2}$ is about 5 per unit redshift (Petitjean et al. 1993). The probability that a randomly placed Ly α cloud with $N(\text{H I}) \sim 10^{16} \text{ cm}^{-2}$ is observed within 200 km s^{-1} from the redshift of G433 along the line of sight to J2233–606 is smaller than 0.01. The absorption may arise in a galaxy which is a member of a group or cluster associated with the quasar. However the covering factor of the galaxies must be large. Indeed a similar situation has been observed along the lines of sight to Q1026–0045A,B, two quasars at $z_{\text{em}} = 1.438$ and 1.520 respectively, with an-

gular separation $36''$, corresponding to transverse linear separations between lines of sight of $\sim 150 h^{-1} \text{ kpc}$ (Petitjean et al. 1998). A metal-poor associated system is seen at $z_{\text{abs}} = 1.4420 \sim z_{\text{em}}^A$ along the line of sight to A, with a complex velocity profile. A strong Ly α absorption is detected along the line of sight to B, redshifted by only 300 km s^{-1} relatively to the associated system in A. It is tempting to interpret these two similar situations as a consequence of the presence of a gaseous disk, halo or other structure of radius larger than $200 h^{-1} \text{ kpc}$ surrounding the foreground quasars. Follow-up studies of the environment of quasar Q433 will be important to check this hypothesis. In particular redshifts are needed for field galaxies in the range $z \sim 1.2$ – 1.5 .

4.2. System at $z_{\text{em}} = 0.5704$ (Galaxy G486)

The line of sight to QSO J2233–606 passes through the disk of a large and bright, approximately face-on, spiral galaxy at an impact parameter of $\sim 18 h^{-1} \text{ kpc}$ ($4.7''$). This is a situation where possibly damped H I absorption, and conspicuous metal absorptions are expected. H I absorption associated with this galaxy is seen in the Lyman series (see Fig. 5) at $z_{\text{abs}} = 0.5704$. Although uncertainties are large, the equivalent widths are consistent with $N(\text{H I}) > 10^{19} \text{ cm}^{-2}$. Because of the poor spectral resolution of the G140L spectrum, the presence of C III $\lambda 977$ and C II $\lambda 1036$ cannot be ruled out. The C IV and Al III doublets are most certainly blended. The strongest constraint on the metal content in the gas comes from the ABSENCE of Fe II $\lambda 2600$ at $\lambda 4083.3$ in the AAT spectrum (Outram et al. 1998) down to $W_{\text{rest}} = 0.02 \text{ \AA}$. Note that Fe II $\lambda 2382$ is lost in a strong Ly α complex. The above limit implies $N(\text{Fe II}) < 1.6 \cdot 10^{12} \text{ cm}^{-2}$, so the inferred gaseous iron metallicity cannot be much more than 0.01 solar. However, iron can be heavily depleted into dust grains and the true metallicity could be much higher. Unfortunately the Mg II wavelength range has not yet been adequately covered. A weak absorption line, seen at $\lambda 4390.66$ in the AAT spectrum, is probably Mg II $\lambda 2796$ at $z=0.57014$ but needs confirmation. A 4σ absorption feature of $EW_{\text{obs}} = 0.14 \text{ \AA}$ is present in a new ESO spectrum at $4401.89 \pm 0.07 \text{ \AA}$, giving $z = 0.57012$ if identified with Mg II $\lambda 2803$ (V. D’Odorico, private communication). This system is potentially very interesting as it would be really surprising if the metal content were confirmed to be so small.

Inside the STIS field, another galaxy (G448 in Table 1) at $29.8''$ to the North-East of J2233–606 is at $z_{\text{em}} = 0.5800$. No associated absorption is seen.

4.3. Other objects

A single component Mg II system is seen at $z_{\text{abs}} = 0.4143$ with $b = 7 \text{ km s}^{-1}$ and $\log N(\text{HI}) = 12.8$ (Outram et al. 1998). The Lyman β line has $W_{\text{rest}} = 1.37 \text{ \AA}$ which corresponds to $\log N(\text{H I}) \sim 19$ for $b = 7 \text{ km s}^{-1}$. We identify two galaxies at a distance smaller than $40''$ (or $130 h^{-1} \text{ kpc}$) from the quasar at redshifts

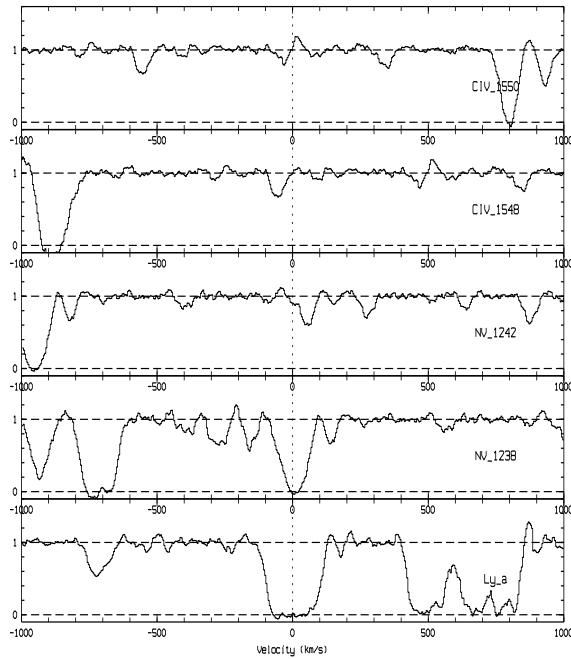


Fig. 4. Absorptions in the $z_{\text{abs}} = 1.3367$ absorption system on a velocity scale in the normalized QSO spectrum. It is probable that the cloud has two subcomponents at $z_{\text{abs}} = 1.3363$ and 1.3368 ($\Delta v \sim 60 \text{ km s}^{-1}$). From bottom to top, H I Ly α , Nv1238, Nv1242, CIV1548, CIV1550.

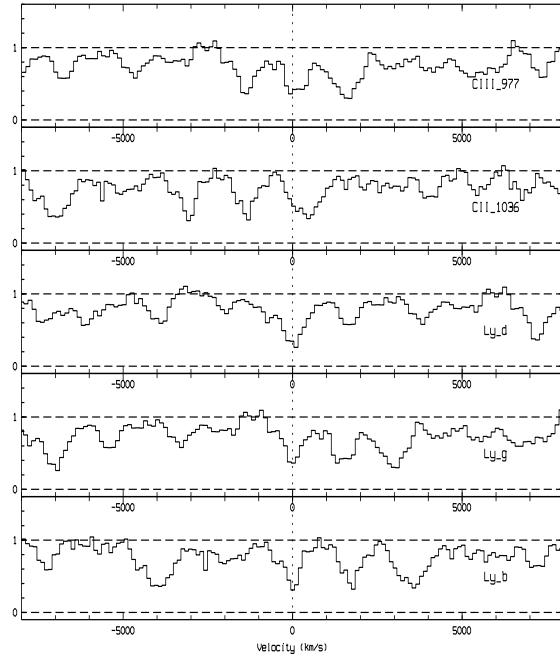


Fig. 5. Absorptions in the $z_{\text{abs}} = 0.5704$ absorption system on a velocity scale. From bottom to top, H I Ly β , Ly γ , Ly δ and CII1036, CIII977.

$z_{\text{em}} \sim 0.4147$ and 0.4148 , (see Table 1), while a third one with $z_{\text{em}} \sim 0.4147$ (G1109) is only slightly outside the $1'$ radius. Number counts simulations indicate that only about 0.5 galaxies brighter than $I = 22$ are expected per square arc minute in the 0.4 – 0.5 redshift range. The over-density of galaxies at this redshift suggests a group or cluster, from which another member, closer to the QSO, could then be responsible for the absorption. A possible candidate is object G484, at a distance of $18.2''$, resolved on the HST image into an interacting pair of spirals (see Fig. 1)

We detect galaxies at $z_{\text{em}} = 0.066$, 0.227 , 0.330 and 0.645 at a distance of 45 , 103 , 170 , and $220 h^{-1}$ kpc from J2233–606. No conspicuous absorption is found at these redshifts, in particular from the Mg II doublet.

5. Conclusions

From spectroscopic observations of galaxies brighter than $I = 21$ around QSO J2233–606 in the HDF-S field, and a search for associated absorption lines in the QSO spectrum, we find that:

(i) Object Q433 (see Table 1) is a quasar at $z = 1.3351$ with $M(I) = -22.8$. The small projected angular separation between the two quasars ($44.5''$) makes this pair an ideal target for QSO environment studies. Indeed strong H I Ly α and Ly β absorptions are seen at $z_{\text{abs}} = 1.3367$ in the spectrum of QSO J2233–606, consistent with a neutral hydrogen column density of $N(\text{H I}) > 10^{16} \text{ cm}^{-2}$. This second HST detection of a Ly α absorption associated with a quasar (see Petitjean et al. 1998) suggests that quasars are surrounded by huge absorbing halos, disks or other structures of radii larger than $200 h^{-1}$ kpc.

(ii) The bright spiral galaxy (J2233378–603324), projected at $4.7''$ from QSO J2233–606, is at $z = 0.5704$. Strong H I absorption is seen in the QSO spectrum. The paucity of metal absorptions, in particular the absence of Fe II absorption, suggests that the disk of this galaxy is metal-poor. However the Mg II absorption range has not been adequately observed yet.

(iii) Galaxies G496 and G1096, at $z = 0.4148$ and 0.4147 respectively, correspond to an MgII absorption system in the QSO spectrum. The over-density of objects at this redshift suggests that another object even closer to the QSO (possibly G484) may be responsible for the absorption.

Acknowledgements. This program has been conducted with partial support by the Training and Mobility of Researcher program under contract number FMRX-CT96-0086: 'The Formation and Evolution of Galaxies'. LT acknowledges financial support by the same program.

References

- Bertin E., and Arnouts S., 1996, A&A 117, 393
- Boyle B. J., 1997, AAO Newsletter, 83, 4
- Dennefeld M., et al., 1999, A&A in preparation
- Francis P. J., Hewett P. C., Foltz C. B., Chaffee F. H., Weymann R. J., Morris S.L. 1991, ApJ 373, 465

Gallego, J., Zamorano J., Aragon-Salamanca A., Rego M. 1995,
ApJ 455, L1

Gardner et al. 1999, in press

Landolt A. U. 1992, AJ., 104, 340

Lilly, S., Tresse, L., Hammer, F., Crampton, D., Le Fèvre, O.
1995, ApJ 455, 108

Outram P. J., Boyle B. J., Carswell R. F., Hewett P.C.,
Williams R. E., Norris R. P., 1998, MNRAS in press (astro-
ph/9809404)

Petitjean P., Webb J. K., Rauch M., Carswell R. F., Lanzetta
K., 1993, MNRAS 262, 499

Petitjean P., Surdej J., Smette A., Shaver P., Mücket M., Remy
M., 1998, A&A 334, L45

Savaglio S., 1998, AJ 116, 1055

Sealey M. K., Drinkwater J. M., Webb J. K., 1998, ApJL 499,
135

Stone R.P.S., and Baldwin J. A., 1984, MNRAS 204, 347

Williams R. E., et al., 1996, AJ. 112, 1335

Williams R. E., et al., 1999, in preparation